Treosulfan pharmacokinetics and dynamics in pediatric allogeneic stem cell transplantation

Stoep, M.Y.E.C. van der

Citation

Stoep, M. Y. E. C. van der. (2022, November 30). *Treosulfan pharmacokinetics and dynamics in pediatric allogeneic stem cell transplantation*. Retrieved from https://hdl.handle.net/1887/3491484

CHAPTER 02

POPULATION PHARMACOKINETICS OF TREOSULFAN IN PEDIATRIC PATIENTS UNDERGOING HEMATOPOIETIC STEM CELL TRANSPLANTATION

M.Y. Eileen C. van der Stoep, Juliette Zwaveling, Alice Bertaina, Franco Locatelli, Henk-Jan Guchelaar, Arjan C. Lankester, Dirk Jan A.R. Moes

ABSTRACT

Aims:

Treosulfan is an alkylating agent increasingly used prior to hematopoietic stem cell transplantation (HSCT). The aim of this study was to develop a population pharmacokinetic model of treosulfan in pediatric HSCT recipients and to explore the effect of potential covariates on treosulfan pharmacokinetics (PK). Also, a limited sampling model (LSM) will be developed to accurately predict treosulfan exposure suitable for a therapeutic drug monitoring setting.

Methods:

In this multicentre study, 91 patients, receiving a total dose of 30, 36 or 42 g/m^2 treosulfan, administered over 3 consecutive days, were enrolled. A population pharmacokinetic model was developed and demographic factors, as well as laboratory parameters, were included as potential covariates. In addition, a LSM was developed using data from 28 patients.

Results:

A two-compartment model with first order elimination best described the data. Bodyweight with allometric scaling and maturation function were identified as significant predictors of treosulfan clearance. Treosulfan clearance reaches 90% of adult values at 4 postnatal years. A model-based dosing table is presented to target an exposure of 1650 mg*hr/L (population median) for different weight and age groups. Samples taken at 1.5, 4 and 7 hours after start of infusion resulted in the best limited sampling strategy.

Conclusions:

This study provides a treosulfan population PK model in children and captures the developmental changes in clearance. A 3-point LSM allows for accurate and precise estimation of treosulfan exposure.

2

INTRODUCTION

Treosulfan is an alkylating agent with both myeloablative and immunosuppressive properties [1]. In the last decade, treosulfan is increasingly being used in conditioning regimens prior to hematopoietic stem cell transplantation (HSCT), in children with both malignant and non-malignant disorders. It has been shown to be effective and has a relatively mild toxicity profile [2-7]. The most commonly reported toxicities are skin, mucosal, gastro-intestinal and hepatic toxicity [4, 6-8].

Treosulfan is an analogue of busulfan, from which it differs for two hydroxyl groups leading to a somewhat different mechanism of action [9]. Treosulfan is a prodrug and is non-enzymatically, pH-dependently converted into a monoepoxide and diepoxide derivative ((S,S)-EDBM and (S,S)-DEB, respectively) [10]. These metabolites are thought to be responsible for DNA alkylation, interstrand DNA crosslinking, chromosomal aberration and, finally, induction of apoptosis [11].

To date, only a few papers have described the clinical pharmacokinetics of treosulfan in children, often based on small sample size datasets [12-18]. Three population pharmacokinetic models in children have been published, including one of our own group (see Supplemental Material 1). However, the sample size of two of the three studies was limited and besides bodyweight (BW), no significant covariates could be identified to explain interindividual variability in pharmacokinetics [16, 17, 19]. Also, the inclusion of infants (children <2 years) was limited; a population particularly of interest because variability and total exposure seems especially high in this subgroup [13, 18].

In order to perform PK-guided dosing and to accurately establish the exposure, intensive blood sampling is required. This may be laborious for both patients and staff employing PK-guided dosing in daily practice. In a pilot study, we reported that a limited sampling model (LSM) based on PK data from 20 pediatric patients based was capable of accurately predicting the area under the concentration-time curve from zero to infinity ($AUC_{0-\infty}$), with a model based approach, requiring only 2 blood samples [17].

The primary aim of the current study is to develop a population pharmacokinetic model of treosulfan in pediatric HSCT recipients with improved predictive performance compared to previously published models using a comprehensive multi-institutional dataset. The secondary aim is to identify patient-related factors that may explain pharmacokinetic variability by means of a covariate analysis. Finally, a limited sampling model will be developed to accurately estimate treosulfan systemic exposure suitable for a therapeutic drug monitoring (TDM) setting.

METHODS

Patient population

All pediatric patients who had participated in a prospective, observational, multicentre study and who had received treosulfan as part of conditioning prior to HSCT between June 2011 and March 2017 in the Leiden University Medical Center (LUMC), The Netherlands, and the Bambino Gesù Children's Hospital (OPBG) in Rome, Italy were included in this population pharmacokinetic analysis. Patients without permanent central venous access were excluded. The LUMC institutional Ethics Committee approved the study protocol (P12.267) which was subsequently approved in OPBG. Written informed consent to participate in the study was obtained from either parents or legal guardian, and patients older than 12 years were asked to give their assent, according to the Helsinki Declaration (last amended in 2013, Fortaleza, Brazil). In line with current dosing recommendations, patients older than 1 year received intravenous treosulfan in a total dose of 42 g/m^2, administered over 3 consecutive days (14 g/m^2 per day, 3-hour infusion). Patients under the age of 1 year received a total dose of 30 g/m^2 or 36 g/m^2 (10 g/m^2 or 12 g/m^2 per day, 3-hour infusion). Patients who underwent a second transplantation (n=7) in which treosulfan was also part of the conditioning regimen were included twice in the analysis. Samples were taken at first and second transplantation. Because the time between first and second transplantation was more than several months, these results were considered as distinct individuals.

Sampling and analysis

For treosulfan PK assessment, blood samples were collected in serum tubes (BD Vacutainer® Plus plastic serum tube) on day 1. In patients who gave additional consent, blood samples were also collected on day 3 to determine intra-patient variability. Samples were collected at 1.5, 3.5, 4, 5, 7 and 9 hours after start of infusion (extensive sampling) or at 4 and 7 hours after start of infusion (limited sampling). Samples were centrifuged as soon as possible (i.e. within 5 hours), and serum stored at -20°C. A validated reversed-phase high-pressure liquid chromatography (RP-HPLC) using ultraviolet (UV) detection was used to determine treosulfan concentration in serum, as previously reported [17]. Briefly, treosulfan and the internal standard busulfan were made detectable through derivatization with sodium diethyldithiocarbamate (DDTC). Linearity was established up to 500 mg/L with a lower limit of quantification (LLOQ) of 6.8 mg/L. Accuracy of quality control (QC) samples was within the 90-110% limit. The intra-day imprecision, expressed as coefficient of variation (CV%), ranged from 2.0% to 3.3% and inter-day imprecision ranged from 2.1% to 2.8%.

Pharmacokinetic modelling

Nonlinear mixed effect modelling was used to estimate pharmacokinetic parameters as implemented in the NONMEM software package (version 7.3.0; Icon Development Solutions, Ellicott City, MD, USA), using PsN toolkit 4.7.0 and Piraña version 2.9.7 as modelling environment. Plotting of the results was performed using statistical software package R (v3.4.4) and R studio Version 1.0.456.

Base model

Initially, a base model was developed without covariates. Plots of observed concentration-time data of treosulfan were examined. One-, two- and three compartmental pharmacokinetic models with first-order elimination were compared to find the optimal fit for the concentration-time data. Interindividual variability (IIV) was assumed to follow a log-normal distribution and was implemented in the model as follows (Eq.1):

$$P_i = P_{POP} \times exp^{\eta_i} \tag{1}$$

where P_i is the pharmacokinetic parameter of ith individual, P_{pop} is the population mean value of the parameters and η_i is a normally distributed random value with mean zero and variance ω^2. In 24 patients, interoccasion variability (IOV) could be evaluated and implemented similarly (Eq. 2) with each dose and subsequent sampling defined as a separate occasion.

$$P_i = P_{POP} \times exp\,(\eta_{1x1} + \eta_{2x2} + \cdots\cdots \eta_{ixi+}) \tag{2}$$

A proportional error model and a combined proportional and additive error model were examined to describe the residual error. Eventually, a proportional error model was implemented as follows (Eq. 3):

$$Y_{ij} = Y_{PREDij} \times (1 + exp_{proportional}) \tag{3}$$

where Y_{ij} is the jth measured concentration in the ith subject, Y_{PREDij} is the predicted concentration based on the model and $exp_{proportional}$ is the proportional error component.

Four of 410 (1%) serum concentration time points were below the lower limit of quantification. These measurements (actual values) were included in the dataset as proposed by Hecht *et al* [20].

Covariate analysis

The parameter values were standardised for a body weight of 70 kg and allometrically scaled (Eq. 4):

$$F_{size} = \left(\frac{BW}{70\,kg}\right)^{\alpha} \tag{4}$$

where F_{size} is the fractional difference in allometrically scaled size compared with a 70 kg individual. When scaling clearance (Cl) and intercompartmental clearance (Q) α is fixed to 0.75 and for volume of distribution of the central (V1) and peripheral compartment (V2) α is fixed to 1 [21].

Furthermore, a sigmoid E_{max} model was used to describe the maturation of treosulfan Cl on postmenstrual age (PMA) as follows (Eq. 5):

$$F_{mat} = \left(\frac{1}{1+\left(\frac{PMA}{TM_{50}}\right)^{-Hill}} \right) \tag{5}$$

where F_{mat} is the fraction of adult treosulfan clearance value, TM_{50} is the PMA at which maturation is 50% of the adult value, and the Hill coefficient is associated with the slope of the developmental profile [22]. PMA was estimated by adding a gestational age of 40 weeks to postnatal age.

Total clearance (Cl_{tot}) could then be described as follows (Eq. 6):

$$Cl_{tot} = Cl_{pop} \times F_{size} \times F_{mat} \tag{6}$$

where Cl_{pop} is the overall population value of parameter. A similar model was used for intercompartmental clearance (Q).

Potential other covariates were chosen based on biological or physiological plausibility and clinical relevance. Assessed covariates included: gender, underlying disease, conditioning regimen, hemoglobin, hematocrit, serum albumin and estimated glomerular filtration rate (eGFR) as a measure of renal function. This was calculated using the revised Schwartz formula (see Supplemental Material 2) and to avoid implausible high eGFR values, these were capped at 120 ml/min/1.73 m^2 [23]. There were no missing covariate values. All preselected covariate relationships were used for a systematic stepwise covariate modelling (SCM), with stepwise forward inclusion and backward deletion [24]. In the forward inclusion and backward deletion, the levels of statistical significance were set at P<0.05 and P<0.01, respectively, corresponding to differences in the NONMEM objective function value (OFV) of 3.84 and 6.64, respectively (1 degree of freedom). A covariate effect was only maintained in the model if the inclusion resulted in reduction of random variability of the PK parameter and improved model fit.

Final model evaluation

Model selection was based on physiological plausibility, visual inspection of goodness-of-fit plots (e.g. observed concentrations versus individual and population-predicted concentrations) and statistical significance. Throughout the model building process, an adjusted model was chosen over the original model if the drop in the objection function value (OFV) [-2 log likelihood] was >6.63 (P<0.01, with 1 degree of freedom, assuming chi-squared [χ^2] distribution). Shrinkage in interindividual variability and residual error were automatically calculated by NONMEM. Values below 30% were deemed acceptable [25]. Evaluation of the precision of the pharmacokinetic parameters was performed with 1000 bootstrap replicates. The stability and performance of the final model were assessed using a prediction-corrected visual predictive check (VPC), since different dosages were used. Prediction-corrected VPC was performed with 1000 replicates by simulating concentrations from the final model with the use of the original dataset. The median and the 10th and 90th percentiles of the simulated concentrations at each time point were calculated and plotted together with the median and the 10th and 90th percentiles of the observed concentrations. The distribution of the observed concentrations was visually compared to the simulated distribution. Differences and overlap of the simulated and original distributions indicated the adequacy of the identified model. In addition, the previously published models by Ten Brink *et al.* [17], Danielak *et al.* [19], and Mohanan *et al.* [16] were compared with the final model to show their ability to describe the current extensive treosulfan PK dataset. The difference in predictive performance was shown by means of comparing the prediction corrected VPCs of the different models.

Simulations to individualize dosing

Based on our final model, individual treosulfan doses were estimated to target an $AUC_{0-\infty}$ of 1650 mg*hr/L, the daily median of treosulfan $AUC_{0-\infty}$ in patients receiving the most common dose of 14 g/m^2. Bayesian pharmacokinetic parameter estimates were obtained by post hoc estimation in NONMEM. $AUC_{0-\infty}$ was then calculated as:

$$AUC_{0-\infty} = \frac{Dose * F}{Cl}$$

(7)

where F is equal to 1.

Clinical covariates were based on the 5th, 50th and 95th percentile estimates of weight per age for boys as provided by the CDC standard growth charts for infants and children [26].

Limited Sampling Model

Patients and data collection

Thirty-five "full" pharmacokinetic profiles from 28 different patients were used to find the optimal limited sampling model for treosulfan. These "full" pharmacokinetic profiles consisted of six blood samples collected over 9 hours (1.5, 3.5, 4, 5, 7 and 9 hours after start of a 3-hour infusion).

Pharmacokinetic and statistical analysis

"True" exposure ($AUC_{full0-\infty}$) was calculated from all measured concentration-time points using post hoc estimation in NONMEM with the final model ((DOSE *F1)/ Cl). Limited sampling model (LSM) predicted AUC ($AUC_{pred0-\infty}$) was calculated by selecting several concentration-time points and combinations of time points. Bias and imprecision were calculated to assess the performance of the different LSMs according to the guidelines proposed by Sheiner and Beal [27]. Formulas can be found in Supplemental Material 2. A Pearson correlation coefficient test was performed to determine the correlation between $AUC_{full0-\infty}$ and $AUC_{pred0-\infty}$.

RESULTS

Patients

A total of 91 pediatric patients were included in this study; 58 were male and 33 female. Patient characteristics are summarized in Table 1. Median age was 4.3 years (range 0.1 - 18.2) and median body weight was 15.6 kg (range 3.8 - 75.0). Seven

patients underwent a second transplantation in which treosulfan was also part of the conditioning regimen. The median time between the first and second transplantation was 8.5 months. The dataset consisted of 410 samples. The concentration-time data were reviewed for completeness and consistency of sampling and dosing times. For distribution of samples, see Supplemental Material 3. Full concentration-time profiles of treosulfan are shown in Figure 1.
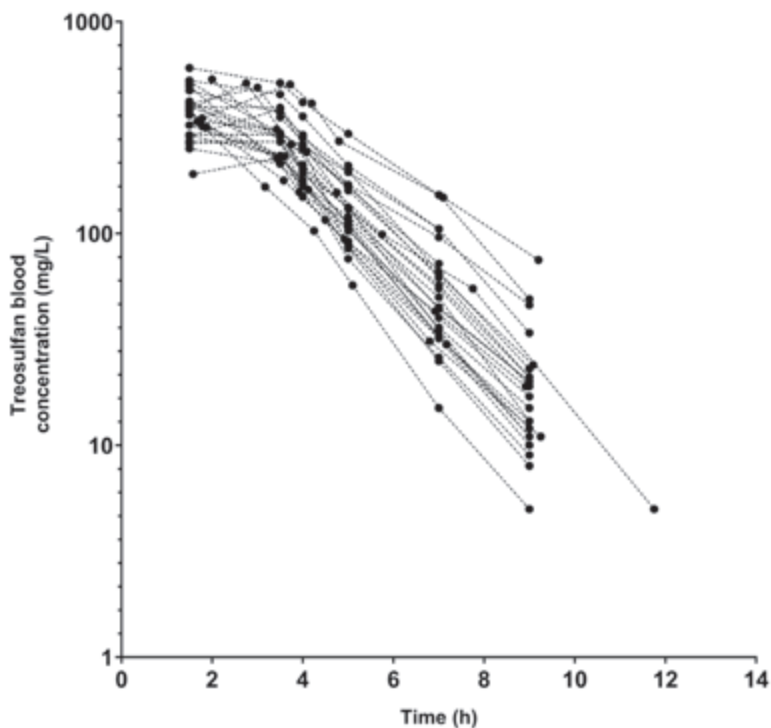

Figure 1. Full concentrations-time profiles of treosulfan in 27 pediatric patients undergoing HSCT, receiving 14 g/m².

Table 1. Patient characteristics (n=91)

2

Characteristic	
Age (years)	4.3 (0.1-18.2)
No. of infants (≤2 years old)	33 (36%)
Bodyweight (kg)	15.6 (3.8-75.0)
BSA (m^2)	0.7 (0.3-1.9)
Gender (% male)	63.7
Creatinine (μmol/L)	26 (8-166)
Albumin (g/L)	38 (20-52)
Hematocrit (L/L)	0.291 (0.199-0.384)
Hemoglobin (mmol/L)	6.6 (4.6-10.5)
eGFR (mL/min/1.73m^2)	111 (16-120)
Underlying disease (*n*)	
Hemoglobinopathy	35 (38.5%)
Hematological malignancy	17 (18.7%)
Primary immune deficiency	26 (28.6%)
Bone marrow failure	11 (12.1%)
Other	2 (2.2%)
No. of transplants (*n*)	
1	84 (92.3%)
>1	7 (7.7%)
Donor (*n*) [a]	
MSD	29 (31.9%)
MUD (≥ 9/10)	41 (45.1%)
MMFD (haplo)	20 (22.0%)
Stem cell source (*n*)[1]	
BM	56 (61.5%)
PBSC	23 (25.3%)
CB	10 (11.1%)
BM + CB	1 (1.1%)
Conditioning regimen (*n*)	
Treo+Flu+Thiotepa	59 (64.8%)
Treo+Flu	29 (31.9%)
Treo+Other (e.g. Mel)	3 (3.3%)
Treosulfan dose (*n*)	
10 g/m^2	16 (17.6%)
12 g/m^2	2 (2.2%)
14 g/m^2	73 (80.2%)
Transplant centre (Leiden/Rome)	63/28
Exposure	
Treosulfan AUC$_{0-\infty}$ (mg*hr/L)	1658 (643-3371)

Data are presented as median (range) unless stated otherwise. [a]: one patient died before transplantation, but after completing conditioning. BSA: body surface area, eGFR: estimated glomerular filtration rate, BM: bone marrow, PBSC: peripheral blood stem cells, CB: cord blood, MSD: matched sibling donor, MMFD: mismatched family donor, MUD: matched unrelated donor, Treo: treosulfan, Flu: fludarabine, Thio: thiotepa, Mel: melphalan, AUC$_{0-\infty}$: area under the curve from zero to infinity

Structural model development

Treosulfan PK was best described by a two-compartment model with first-order elimination from the central compartment. Adding the second compartment showed a significant improvement compared to the one-compartment model (ΔOFV = -127.78). The two-compartment model was parameterized in terms of volume of distribution of the central (V1) and peripheral (V2) compartment, and clearance from the central compartment (Cl) and intercompartmental clearance between V1 and V2 (Q). The base model showed the following PK parameters: average clearance (Cl) of 5.94 L/h (CV: 79.9%), average central distribution volume (V1) of 0.77 L (CV: 141.4%), average peripheral distribution volume (V2) of 8.73 L (CV: 90.5%) and average inter-compartmental clearance (Q) of 24.6 L/h (CV: 128.5%).

Covariate model

A bodyweight-based allometric model was added to all clearance and volume of distribution parameters and significantly improved the model (ΔOFV = -90.22). The addition of maturation of treosulfan Cl based on PMA on Cl and Q improved the model even further (ΔOFV = -39.63). The maturation of treosulfan clearance reaches 50% of adult values at 38 weeks PMA, that is 2 weeks prior to birth assuming a full-term gestational age of 40 weeks. Clearance reaches 90% of adult values at approximately 4 years old (Figure 2). In the stepwise covariate modelling process, eGFR was found to be a significant covariate on Cl (ΔOFV = -16.72), but the VPC worsened when eGFR was incorporated in the model and interindividual variability of the PK parameters increased. Therefore, we decided not to include eGFR to the model and only incorporate bodyweight and maturation of clearance in the final model.
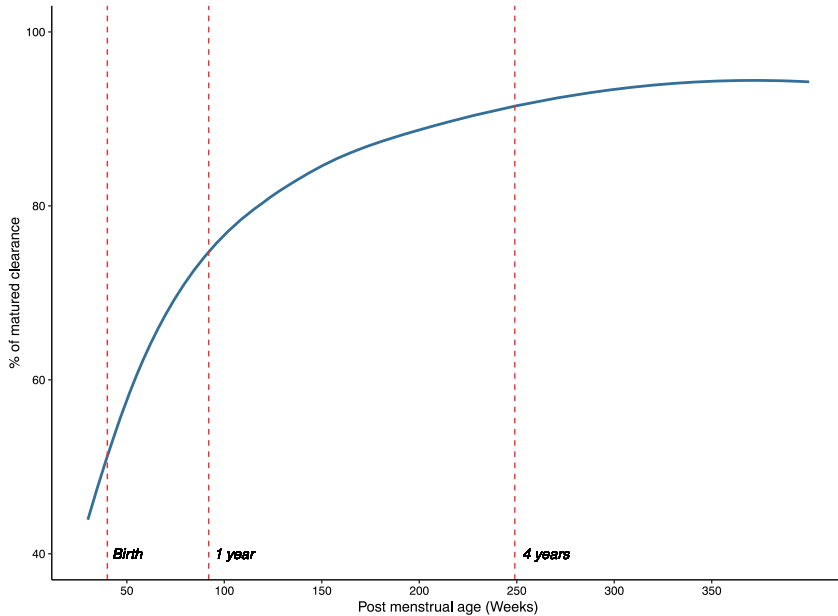
2

Figure 2. Maturation of treosulfan clearance as percentage of adult values.

Model evaluation

Parameter estimates of the base model, the model with only allometric scaling and the final model are presented in Table 2. Diagnostic plots of the final model are shown in Figure 3. The final model file code is provided in Supplemental Material 4. The relative standard error for the estimated V2 and Q IIV was over 100%, 201% and 153% respectively. Interestingly, this was not seen when parameters were normalized to the median weight (15.6 kg) (RSE 53% and 46% for V2 and Q respectively, data not shown). However, evaluation with a bootstrap procedure with 1000 bootstrap replicates showed estimates that are in line with the estimates of the PK parameters and their random variability of the final model. The prediction-corrected VPC confirmed an acceptable agreement between the observed data and model-based simulated values (Figure 4A). The median PK parameter estimates and 95% confidence intervals (CI) from the bootstrap analysis are presented in Table 2.

Table 2. Summary of model parameter estimates

Parameter	Base model			Model with allometric scaling			Final model			1000 Bootstrap runs	
	Estimate	RSE (%)	Shr. (%)	Estimate	RSE (%)	Shr. (%)	Estimate	RSE (%)	Shr. (%)	Median value	95% CI
Cl (L/h)	5.94	6		15.9[a]	5		18.8[a]	7		19.4[a]	16.6 - 26.2
V1 (L/)	0.77	17		18.8[a]	17		20.2[a]	18		19.8[a]	5.1 - 29.6
Q(L/h)	24.6	26		17.3[a]	28		21.3[a]	31		22.0[a]	9.7 - 68.9
V2 (L)	8.73	10		16.8[a]	14		16.8[a]	16		16.8[a]	10.9 - 29.6
Hill							1.2	34		1.1	0.3 - 3.2
TM_{50}							38	19		43	22.2 - 74.4
Inter-individual variability											
Cl (CV%)	79.9	11	1	36.9	11	11	31.8	13	15	31.4	22.8 - 40.2
V1 (CV%)	141.4	16	4	45.5	42	20	45.9	42	26	48.4	24.9 - 87.1
V2 (CV%)	90.5	14	2	15.7	208	19	17.3	201	19	20.7	9.1 - 46.0
Q(CV%)	128.5	22	17	45.5	103	21	41.4	153	24	43.3	15.7 - 77.4
Interoccasion variability											
Cl (CV%)	13.1	21	32	13.3	22	38	13.9	23	27	13.0	9.8 - 17.1
Residual variability											
σ (proportional error)	11.8	7	30	12.4	7	27	12.3	4	27	12.0	9.4 - 14.6

Cl = clearance; CV = coefficient of variation; Hill = Hill coefficient for maturation, Q = intercompartmental clearance; RSE = relative standard error; Shr.= shrinkage; TM50 = postmenstrual age at 50% maturation; V1 = volume of distribution of central compartment; V2 = volume of distribution of peripheral compartment; [a] normalised to a bodyweight of 70 kg
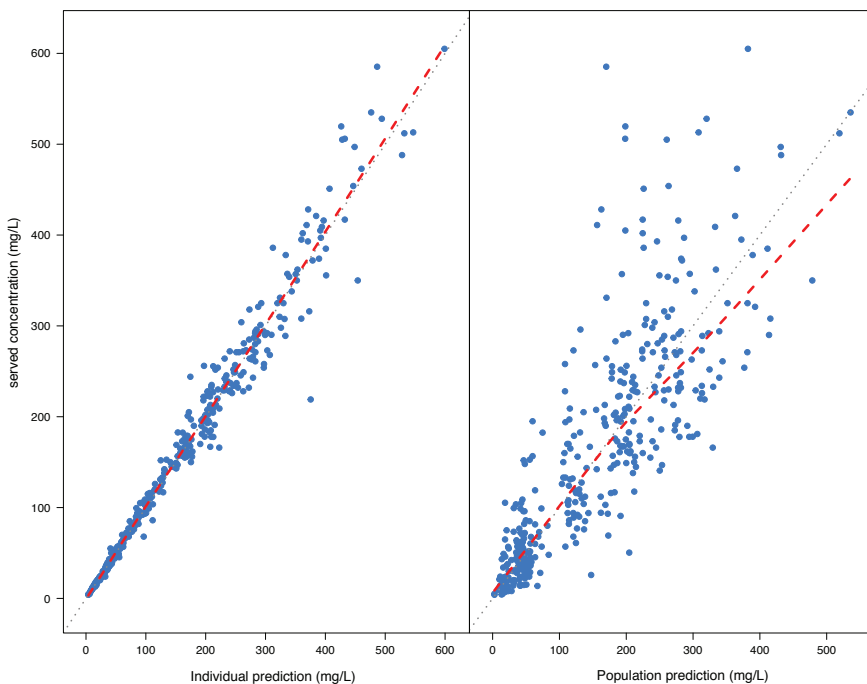
Figure 3. Goodness-of-fit plots for the final pharmacokinetic model. *Left:* individual-predicted concentrations versus observed concentrations. *Right:* population-predicted concentrations versus observed concentrations. Blue dots represent the observations and the red dashed line is a local regression fit of these values. Grey dashed line is the line of unity.

Comparison with previously published population pharmacokinetic models

Our model accounted for age and size differences over a big age range in children (1 month - 18 years). To evaluate the prediction accuracy in children, we performed prediction corrected VPCs with the previously published treosulfan pharmacokinetic models (Figure 4B, C and D) build on pediatric data [16, 17, 19]. The prediction corrected VPCs show that all three models show poor predictions and are not able to properly describe the current dataset.
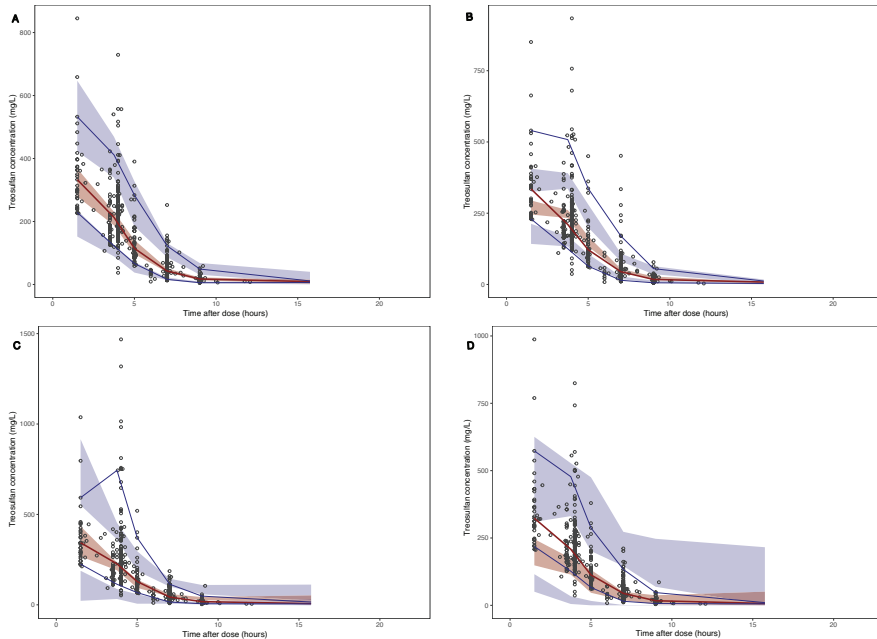
Figure 4. Prediction corrected visual predictive check with median, 10th and 90th observation percentile. The observed treosulfan serum concentrations are shown as open circles. The red and blue lines represent the observed median and 10th and 90th percentile. The shaded areas represent the 95% confidence interval around each of the prediction percentiles. A: present study, B: Ten Brink *et al.*, C: Danielak *et al.*, D: Mohanan *et al.*

Simulations to individualize dosing

The derived population PK parameters from our model were used to calculate the required treosulfan dose to reach an $AUC_{0-\infty}$ of 1650 mg*hr/L (median estimated $AUC_{0-\infty}$ in our cohort) for a set of virtual patients (normal weight and age range). In Table 3, the treosulfan dose per day required to target an $AUC_{0-\infty}$ of 1650 mg*hr/L can be found for each age category for the three different corresponding normal weight percentiles (5th, 50th, 95th). Figure 5 shows that the amount of treosulfan required varies per age, indicated as the grey ribbon between the dotted lines. The recommended treosulfan dose per kg is lower in early years of life and reaches a maximum at

approximately 4 years accounting for maturation of clearance and because dose per kg is higher in younger children based on allometric theory (Figure 5A). Figure 5B shows the absolute treosulfan dose, increasing with age and weight, but with a steeper slope in the beginning accounting for maturation.

Table 3. Recommended treosulfan dose for different age and weight categories (5th, 50th and 95th percentile)

| Age	Weight (kg)	Treosulfan dose (mg) per day	Age	Weight (kg)	Treosulfan dose (mg) per day
0 months	2.6	1350	8 years	20.7	11900
	3.3	1600		25.8	14000
	4.2	1950		35.3	17700
3 months	5.2	2650	9 years	22.7	12800
	6.4	3100		28.7	15250
	7.7	3550		40.4	19700
6 months	6.6	3500	10 years	24.9	13800
	7.9	4000		32.1	16700
	9.5	4600		46.2	21900
9 months	7.4	4100	11 years	27.5	14900
	8.9	4700		36.1	18300
	10.6	5300		52.6	24200
1 year	8.1	4600	12 years	30.6	16200
	9.6	5200		40.7	20000
	11.5	6000		59.3	26600
2 years	10.1	6100	13 years	34.2	17600
	12.2	7000		45.8	22000
	14.7	8000		66.1	28900
3 years	12.0	7300	14 years	38.5	19300
	14.3	8300		51.2	24000
	17.3	9600		72.7	31100
4 years	13.6	8250	15 years	43.0	21000
	16.3	9450		56.5	25800
	20.3	11100		78.8	33100
5 years	15.2	9100	16 years	47.3	22600
	18.5	10500		61.1	27400
	23.5	12700		84.3	34900
6 years	16.9	10000	17 years	50.8	23900
	20.8	11700		64.7	28700
	27.0	14250		88.8	36300
7 years	18.7	11000	18 years	53.2	24800
	23.2	12800		67.3	29500
	30.9	16000		92.0	37400
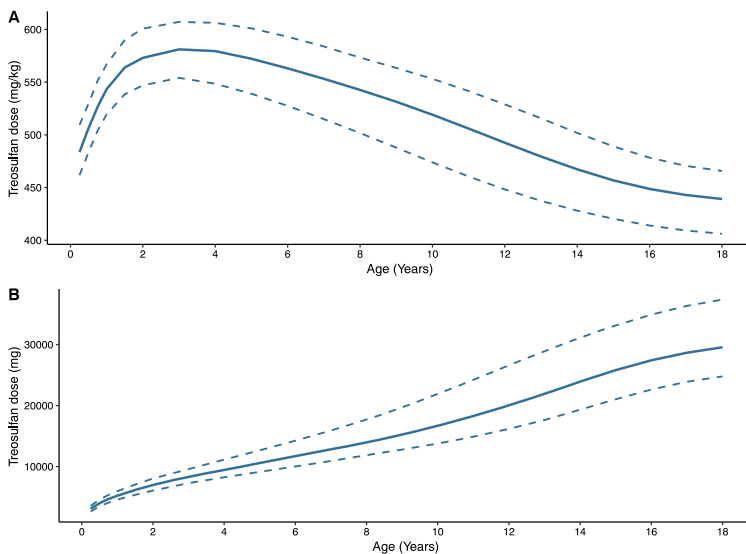
Figure 5. Required treosulfan daily dose in order to obtain a median $AUC_{0-\infty}$ of 1650 mg*hr/L against age **A**: in mg/kg and **B**: absolute dose (mg). The solid line represents the 50th weight percentile for that age, the upper dashed line represents the 5th weight percentile and the lower dashed line represents the 95th weight percentile.

Limited sampling model

The results of the LSM are shown in Table 4 and Figure 6. Predictive performance measurements used are: correlation, percentages of predicted AUCs within 10, 15 and 20% range of the 'true' $AUC_{0-\infty}$ and different ways of describing bias (mean prediction error, MPE; mean percentage prediction error, MPPE) and precision (root mean squared prediction error, RSME; mean absolute percentage predictive error, MAPE). Figure 6 shows results of four LSMs, including both regression lines with 95% confidence intervals as measurements of predictive performance. The best two-point markers were T=4 and 7 hours (R^2 = 0.97, MAPE = 5.06%, MPPE = 0.59%), with 97% of $AUC_{pred0-\infty}$ falling within 15% range of $AUC_{full0-\infty}$. The best three-point marker was T=1.5, 4 and 7 hours (R^2 = 0.99, MAPE = 2.84%, MPPE = -0.05%), with 100% of $AUC_{pred0-\infty}$ falling within 15% and even within 10% range of $AUC_{full0-\infty}$. With the tested single-point marker (T=1.5), prediction performance is far less compared to the two- and three-point markers. The percentage of $AUC_{pred0-\infty}$ that lies within 15% range of $AUC_{full0-\infty}$ is 69%. Population prediction without sampling has a very poor predictive performance and less than 35% of $AUC_{pred0-\infty}$ lies within the 15% range of $AUC_{full0-\infty}$.

2

Table 4. Limited sampling schemes based on one or multiple time points

Time points blood sampling	R^2 pearson	Percentage of AUC_{pred} within 10% range of AUC_{full}	Percentage of AUC_{pred} within 15% range of AUC_{full}	Percentage of AUC_{pred} within 20% range of AUC_{full}	MPE (mg*hr/L)	MPPE (%)	RMSE (mg*hr/L)	MAPE (%)
No sampling (population prediction)	0.01	22.86	31.43	40.00	-52.60	4.23	543.45	23.83
T=1.5	0.67	54.29	68.57	82.86	-29.17	0.41	291.71	11.65
T=4 / 7	0.97	91.43	97.14	100	11.01	0.59	101.79	5.06
T=1.5 / 3.5	0.93	77.14	94.29	97.14	-26.76	-0.66	138.88	5.62
T=5 / 7 / 9	0.96	82.86	94.29	100	-6.23	-0.49	112.20	5.86
T=3.5 / 4 / 7	0.96	82.86	97.14	100	-0.81	-0.06	103.74	5.07
T=1.5 / 3.5 / 4	0.97	91.43	97.14	100	-2.86	0.53	100.09	3.92
T=4 / 5 / 7	0.97	91.43	100	100	2.54	0.13	89.83	4.82
T=1.5 / 4 / 5	0.98	97.14	100	100	-9.00	0.01	77.84	3.28
T=1.5 / 4 / 7	0.99	100	100	100	0.61	-0.05	61.62	2.84
T=1.5 / 3.5 / 4 / 5	0.99	100	100	100	-7.91	0.01	61.93	2.41
T=1.5 / 4 / 5 / 7 / 9	0.99	100	100	100	-0.67	-0.07	45.98	1.91
T=1.5 / 3.5 / 4 / 7 / 9	1.00	100	100	100	1.43	0.06	18.72	0.82

AUC_{pred}: Predicted area under the curve; AUC_{full}: Full or 'true' area under the curve; MPE: Mean prediction error; MPPE: Mean percentage prediction error; RMSE: Root mean squared prediction error; MAPE: Mean absolute percentage predictive error
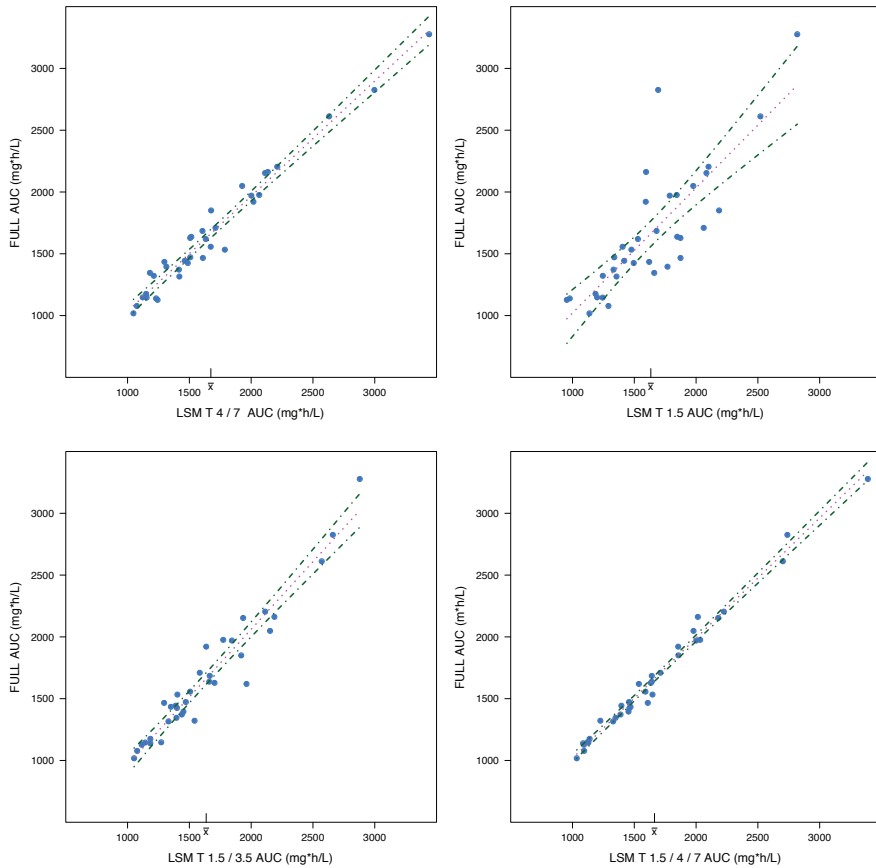
Figure 6. Regression line *(dotted lines)* plots of different limited sampling methods with 95% confidence intervals *(dot-dashed lines)*. *Upper left*: predictive performance of T=4 and 7 as limited sampling model; *upper right*: predictive performance of T=1.5 as limited sampling model; *lower left*: predictive performance of T=1.5 and 3.5 as limited sampling model; *lower right*: predictive performance of T=1.5, 4 and 7 as limited sampling model.

DISCUSSION

In this study, the population PK of treosulfan in pediatric HSCT recipients was best described by a two-compartment model. Allometric scaling of all parameters using BW and the addition of a maturation function using PMA was found to best account for differences in size and age. Other covariates such as gender, underlying disease, conditioning regimen, hematocrit and serum albumin did not significantly influence treosulfan PK. Estimated glomerular filtration rate seems to influence treosulfan PK, because it is known from literature that up to 39% of treosulfan is excreted via the kidneys in unchanged form [28-30]. However, addition of this covariate led to an increased IIV and the prediction corrected VPC worsened compared to the model with bodyweight and maturation of clearance only. Therefore, we ultimately chose not to include this covariate in the final model. In our dataset, only a few patients had an eGFR below 60 ml/min/1.73m^2 (n=5). It is likely that this number might be insufficient to establish this potential relationship accurately.

Danielak *et al.* also studied covariates, but only weight and gender were examined with weight being a significant covariate [19]. Mohanan *et al.* considered more covariates such as age, body weight, BSA, sex, liver size, liver fibrosis and biochemical parameters [16]. Interestingly, none of these variables explained the wide IIV in their cohort. Our model was based on a larger PK dataset, accounting for a wide age range in children (1 month – 18 years) which allows us to incorporate a maturation component in the model and account for maturation of clearance in the first years of life. Treosulfan clearance reaches 90% of adult values at 4 postnatal years.

The parameter estimations obtained in this study are somewhat comparable to the other published models in terms of clearance, but differ in terms of intercompartmental clearance, and the volume of distribution parameters. However, comparison is rather difficult when the values are not reported in a standardized fashion. Standardizing to a bodyweight of 70 kg increased the RSE of IIV of V2 and Q in our model. However, evaluation with a bootstrap procedure with 1000 bootstrap replicates showed estimates that are in line with the estimates of the PK parameters and their random variability

of the final model. Standardizing to the median weight might be more appropriate, because standardizing to a weight outside the observed weight range can increase uncertainty of parameter estimates [31]. On the other hand, comparison with other models is more difficult when standardizing to the median weight, so in the final model the PK parameters were standardized to 70 kg. As we compared the prediction corrected VPCs of the current model versus the models of Ten Brink *et al.*, Danielak *et al.* Mohanan *et al.* it is clear that the current model has superior predictive performance both in the high and low concentration range.

The present study shows a model-based individualized dosing table of treosulfan, aiming for an $AUC_{0-\infty}$ of 1650 mg*hr/L, which was the median exposure of our population. The recommended treosulfan dose is dependent on age and weight. An increase in treosulfan daily dose per kg until the age of 4 years can be seen, reflecting the maturation of clearance and allometry. Recently we showed that there is a relationship between treosulfan exposure and early toxicity [18]. Patients with an exposure >1650 mg*hr/L have an increased risk of developing grade 2 or higher mucositis and skin toxicity. Our model could be used to establish the initial dose, prior to or during treosulfan administration to facilitate therapeutic drug monitoring and thereby prevent toxicity. Little is known about the relationship between treosulfan exposure and transplant outcome parameters yet; however, the study of Mohanan *et al.* reported an association between treosulfan clearance <7.97 L/h/m² and poor overall survival [HR 2.7; CI (1.09-6.76), p=0.032] and event-free survival [HR 2.4; CI (0.98-5.73), p=0.055] in 87 pediatric patients with thalassemia major undergoing HSCT [16]. More studies conducted in different disease settings are needed to establish how systemic exposure to treosulfan can influence patient outcome. Subsequently, the optimal target exposure can then be established.

We also studied a limited sampling strategy, which potentially minimizes the burden of sampling and is convenient for performing TDM in the future. Ten Brink *et al.* chose two time points at 4 and 7 hours after start of infusion, although MPE and MAPE values of the T=1.5 and 5 hours strategy were slightly better [17]. This was

2

done because of practical reasons to avoid sampling during infusion. In the current study, with the addition of new samples, a preference for sampling at T =1.5 hours besides a sample after infusion was shown. This results in 100% of predicted $AUC_{0-\infty}$ falling within 15% and even within 10% radius of full $AUC_{0-\infty}$. We recommend to add a sample at T = 1.5 hours to the two-sample strategy of 4 and 7 hours after infusion, not only to increase predictive performance, but also to make a TDM protocol more robust. For instance, if in clinical practice one of the samples needs to be discarded due to unforeseen sampling or storage errors one would still be able to accurately estimate the $AUC_{0-\infty}$.

Our study has some limitations. Our dataset consisted of rich (full curves) and sparse (2 point curves) data combined together, which is less useful for non-compartmental analysis. However, the current approach of population pharmacokinetics, using nonlinear mixed effects modelling, allows data from a variety of unbalanced sparse and rich data to be analysed. Moreover, drug levels of concomitantly given drugs (such as fludarabine and thiotepa), which might influence treosulfan pharmacokinetics, were not available. In addition, because treosulfan is a prodrug, the active metabolites could be of interest to incorporate in the population pharmacokinetic model. Danielak *et al.* found a weak correlation between exposure to treosulfan and the metabolite S,S-EBDM (r = 0.1681, p < 0.0001). Also, patients with treosulfan exposure above 1650 mg*hr/L were most likely to have a high S,S-EBDM exposure [32]. These issues should be addressed in future studies. We have capped the eGFR values at 120 ml/min/1.73m^2, which could introduce a bias. However, renal function was not a significant predictor for treosulfan clearance and therefore was not of influence in our analysis.

In conclusion, a two-compartment population PK model to describe the serum concentration-time profiles of intravenously administered treosulfan was developed. Bodyweight and age (as PMA) have been identified as significant and clinically relevant covariates influencing treosulfan PK. Treosulfan serum concentrations at 1.5, 4 and 7 hours after start of infusion can be used to accurately estimate treosulfan exposure, particularly in a TDM setting.

ACKNOWLEDGEMENTS.

SOURCE OF FUNDING.

REFERENCES

1. Sjoo F, Hassan Z, Abedi-Valugerdi M, Griskevicius L, Nilsson C, Remberger M, et al. Myeloablative and immunosuppressive properties of treosulfan in mice. Exp Hematol. 2006;34(1):115-21.

2. Beier R, Schulz A, Honig M, Eyrich M, Schlegel PG, Holter W, et al. Long-term follow-up of children conditioned with Treosulfan: German and Austrian experience. Bone Marrow Transplant. 2013;48(4):491-501.

3. Bernardo ME, Piras E, Vacca A, Giorgiani G, Zecca M, Bertaina A, et al. Allogeneic hematopoietic stem cell transplantation in thalassemia major: results of a reduced-toxicity conditioning regimen based on the use of treosulfan. Blood. 2012;120(2):473-6.

4. Boztug H, Zecca M, Sykora KW, Veys P, Lankester A, Slatter M, et al. Treosulfan-based conditioning regimens for allogeneic HSCT in children with acute lymphoblastic leukaemia. Ann Hematol. 2015;94(2):297-306.

5. Mathews V, George B, Viswabandya A, Abraham A, Ahmed R, Ganapule A, et al. Improved clinical outcomes of high risk beta thalassemia major patients undergoing a HLA matched related allogeneic stem cell transplant with a treosulfan based conditioning regimen and peripheral blood stem cell grafts. PLoS One. 2013;8(4):e61637.

6. Morillo-Gutierrez B, Beier R, Rao K, Burroughs L, Schulz A, Ewins AM, et al. Treosulfan-based conditioning for allogeneic HSCT in children with chronic granulomatous disease: a multicenter experience. Blood. 2016;128(3):440-8.

7. Slatter MA, Boztug H, Potschger U, Sykora KW, Lankester A, Yaniv I, et al. Treosulfan-based conditioning regimens for allogeneic haematopoietic stem cell transplantation in children with non-malignant diseases. Bone Marrow Transplant. 2015;50(12):1536-41.

8. Bernardo ME, Zecca M, Piras E, Vacca A, Giorgiani G, Cugno C, et al. Treosulfan-based conditioning regimen for allogeneic haematopoietic stem cell transplantation in patients with thalassaemia major. Br J Haematol. 2008;143(4):548-51.

9. ten Brink MH, Zwaveling J, Swen JJ, Bredius RG, Lankester AC, Guchelaar HJ. Personalized busulfan and treosulfan conditioning for pediatric stem cell transplantation: the role of pharmacogenetics and pharmacokinetics. Drug discovery today. 2014;19(10):1572-86.

10. Feit PW, Rastrup-Andersen N, Matagne R. Studies on epoxide formation from (2S,3S)-threitol 1,4-bismethanesulfonate. The preparation and biological activity of (2S,3S)-1,2-epoxy-3,4-butanediol 4-methanesulfonate. J Med Chem. 1970;13(6):1173-5.

11. Hartley JA, O'Hare CC, Baumgart J. DNA alkylation and interstrand cross-linking by treosulfan. Br J Cancer. 1999;79(2):264-6.

12. Danielak D, Twardosz J, Kasprzyk A, Wachowiak J, Kalwak K, Glowka F. Population pharmacokinetics of treosulfan and development of a limited sampling strategy in children prior to hematopoietic stem cell transplantation. Eur J Clin Pharmacol. 2018;74(1):79-89.

13. Glowka F, Kasprzyk A, Romanski M, Wrobel T, Wachowiak J, Szpecht D, et al. Pharmacokinetics of treosulfan and its active monoepoxide in pediatric patients after intravenous infusion of high-dose treosulfan prior to HSCT. Eur J Pharm Sci. 2015;68:87-93.

14. Glowka FK, Karazniewicz-Lada M, Grund G, Wrobel T, Wachowiak J. Pharmacokinetics of high-dose i.v. treosulfan in children undergoing treosulfan-based preparative regimen for allogeneic haematopoietic SCT. Bone Marrow Transplant. 2008;42 Suppl 2:S67-70.

15. Koyyalamudi SR, Kuzhiumparambil U, Nath CE, Byrne JA, Fraser CJ, O'Brien TA, et al. Development and Validation of a High Pressure Liquid Chromatography-UV Method for the Determination of Treosulfan and Its Epoxy Metabolites in Human Plasma and Its Application in Pharmacokinetic Studies. J Chromatogr Sci. 2016;54(3):326-33.

16. Mohanan E, Panetta JC, Lakshmi KM, Edison ES, Korula A, Na F, et al. Pharmacokinetics and Pharmacodynamics of Treosulfan in Patients With Thalassemia Major Undergoing Allogeneic Hematopoietic Stem Cell Transplantation. Clin Pharmacol Ther. 2018;104(3):575-83.

17. Ten Brink MH, Ackaert O, Zwaveling J, Bredius RG, Smiers FJ, den Hartigh J, et al. Pharmacokinetics of treosulfan in pediatric patients undergoing hematopoietic stem cell transplantation. Ther Drug Monit. 2014;36(4):465-72.

18. van der Stoep M, Bertaina A, Ten Brink MH, Bredius RG, Smiers FJ, Wanders DCM, et al. High interpatient variability of treosulfan exposure is associated with early toxicity in paediatric HSCT: a prospective multicentre study. Br J Haematol. 2017;179(5):772-80.

19. Danielak D, Twardosz J, Kasprzyk A, Wachowiak J, Kalwak K, Glowka F. Population pharmacokinetics of treosulfan and development of a limited sampling strategy in children prior to hematopoietic stem cell transplantation. Eur J Clin Pharmacol. 2017.

20. Hecht M, Veigure R, Couchman L, CI SB, Standing JF, Takkis K, et al. Utilization of data below the analytical limit of quantitation in pharmacokinetic analysis and modeling: promoting interdisciplinary debate. Bioanalysis. 2018;10(15):1229-48.

21. Anderson BJ, Holford NH. Understanding dosing: children are small adults, neonates are immature children. Arch Dis Child. 2013;98(9):737-44.

22. Anderson BJ, Holford NH. Mechanistic basis of using body size and maturation to predict clearance in humans. Drug Metab Pharmacokinet. 2009;24(1):25-36.

23. Schwartz GJ, Work DF. Measurement and estimation of GFR in children and adolescents. Clin J Am Soc Nephrol. 2009;4(11):1832-43.

24. Jonsson EN, Karlsson MO. Automated covariate model building within NONMEM. Pharm Res. 1998;15(9):1463-8.

25. Savic RM, Karlsson MO. Importance of shrinkage in empirical bayes estimates for diagnostics: problems and solutions. The AAPS journal. 2009;11(3):558-69.

26. CDC National Center for Health Statistics - Clinical Growth Charts [updated June 16, 2017. Available from: www.cdc.gov/growthcharts/clinical_charts.htm.

27. Sheiner LB, Beal SL. Some suggestions for measuring predictive performance. J Pharmacokinet Biopharm. 1981;9(4):503-12.

28. Scheulen ME, Hilger RA, Oberhoff C, Casper J, Freund M, Josten KM, et al. Clinical phase I dose escalation and pharmacokinetic study of high-dose chemotherapy with treosulfan and autologous peripheral blood stem cell transplantation in patients with advanced malignancies. Clin Cancer Res. 2000;6(11):4209-16.

29. Beelen DW, Trenschel R, Casper J, Freund M, Hilger RA, Scheulen ME, et al. Dose-escalated treosulphan in combination with cyclophosphamide as a new preparative regimen for allogeneic haematopoietic stem cell transplantation in patients with an increased risk for regimen-related complications. Bone Marrow Transplant. 2005;35(3):233-41.

30. Nemecek ER, Guthrie KA, Sorror ML, Wood BL, Doney KC, Hilger RA, et al. Conditioning with treosulfan and fludarabine followed by allogeneic hematopoietic cell transplantation for high-risk hematologic malignancies. Biol Blood Marrow Transplant. 2011;17(3):341-50.

31. Goulooze SC, Voller S, Valitalo PAJ, Calvier EAM, Aarons L, Krekels EHJ, et al. The Influence of Normalization Weight in Population Pharmacokinetic Covariate Models. Clin Pharmacokinet. 2019;58(1):131-8.

32. Danielak D, Kasprzyk A, Wrobel T, Wachowiak J, Kalwak K, Glowka F. Relationship between exposure to treosulfan and its monoepoxytransformer - An insight from population pharmacokinetic study in pediatric patients before hematopoietic stem cell transplantation. Eur J Pharm Sci. 2018;120:1-9.

Supplemental Material 1. Existing population pharmacokinetic models

Author	Patient population	Treosulfan dose and infusion length	Sampling & quantitation	Model	Pharmacokinetic parameters	Covariates
Present study	N = 91 (64% male) Age (y): 4.3 (0.1–18.2) Weight (kg): 15.6 (3.8–75.0) BSA (m2): 0.7 (0.3–1.9) Disease: Malignant 19%, non-malignant 81%	14 g/m^2 – 3h	1.5, 3.5, 4, 5, 7, 9 h or 4, 7 h after start infusion HPLC-UV	Population (two-compartment)	Cl: 18.8 L/h/70 kg Q: 21.3 L/h/70 kg V1: 20.2 L/70 kg V2: 16.8 L/70 kg	Weight, age
Ten Brink (17)	N = 20 (65% male) Age (y): 4.4 (1.1–16.7) Weight (kg): 15.6 (9.3–52.0) BSA (m2): 0.61 (0.01–1.49) Disease: Malignant 20%, non-malignant 80%	14 g/m^2 – 3h	1.5, 3.5, 4, 5, 7, 9 h after start infusion HPLC-UV	Population (one-compartment)	Cl: 6.85 L/h/20 kg V: 13.2 L/20 kg	Weight
Danielak (12)	N = 15 (80% male) Age (y): 7.8 (0.4–15) Weight (kg): 26.9 (7.7–52) BSA (m2): 0.95 (0.25–1.63) Disease: Malignant 67%, non-malignant 33%	10 g/m^2 – 1h, n = 1 12 g/m^2 – 2h, n = 4 14 g/m^2 – 2h, n = 4 12 g/m^2 – 1h, n = 6	7 patients: 0.5, 1, 3, 4, 6, 8 h after start infusion 8 patients: 0.5, 1, 1.5, 2, 2.5, 3, 4, 5, 8, 12 h after start infusion HPLC-MS/MS	Population (two-compartment)	Cl: 14.7 L/h/70 kg Q: 2.25 L/h V1: 26.0 L/70 kg V2: 9.93 L/70 kg	Weight
Mohanan (16)	N = 87 (63% male) Age (y): 9.0 (1.5–25) Weight (kg): 23.2 (11.4–55.0) BSA (m2): 0.93 (0.48–1.56) Disease: Thalassemia Major only	14 g/m^2 – 5 g/h	0h, end of infusion, 1, 2, 3, 5, 7, 24 h after end of infusion UPLC-RID	Population (two-compartment)	Cl: 11.6 L/h/m^2 Q: 2.14 L/h/m^2 V1: 19.4 L/m^2 V2: 2.01 L/m^2	-

Supplemental Material 2. Formulas

Demographic covariate formulas:

Estimated Glomerular Filtration Rate (Schwartz Equation):

$$eGFR = \frac{0.413 \ \times Height \ (cm)}{Serum \ creatinine}$$

BSA (Mosteller (1987)):

$$BSA \ (m^2) = \sqrt{\frac{Height \ (cm) \times Weight \ (kg)}{3600}}$$

Limited sampling strategy statistical analysis formulas:

Bias

$$Mean \ prediction \ error \ (MPE) = mean \ (AUC_{pred} - AUC_{full})$$

$$Mean \ percentage \ prediction \ error \ (MPPE) = mean \ (\frac{AUC_{pred} - AUC_{full}}{AUC_{full}} \times 100\%)$$

Imprecision

$$Root \ mean \ squared \ prediction \ error \ (RMSE) = \sqrt{mean \ (AUC_{pred} - AUC_{full})^2}$$

$$Mean \ absolute \ percentage \ prediction \ error \ (MAPE)$$
$$= mean \ (\frac{|AUC_{pred} - AUC_{full}|}{AUC_{full}} \times 100\%)$$

The percentage of AUC_{pred} within a x% radius of AUC_{full} is decreased by both greater bias and worse precision and is therefore a useful measure of overall predictive ability.

Supplemental Material 3. Distribution of collected samples

Time after start of infusion	Number of samples
1.5	39
3.5	45
4	115
5	47
6	10
7	105
8	4
9	41
10	2
12	2

Supplemental Material 4. Model file

;; Description: PK of treosulfan, 2 cmt model IV infusion

$PROBLEM PK of treasulfan,2 cmt model IV infusion

$INPUT   ID TAD TIME DV AMT DOSE TEST AGE WT RATE ISM

    CLCR CREAT CMT EVID DAY BSA ULD ULD2 COND

    ALB HB HT PH PMA

$DATA   TREOSULFAN.csv IGNORE=#

$SUBROUTINE ADVAN6 TOL=3

$MODEL   COMP=(CENTRAL) COMP=(PERI)

$PK

DAY1=0

```
DAY2=0

DAY3=0

IF(DAY.EQ.1)DAY1=1

IF(DAY.EQ.2)DAY2=1

IF(DAY.EQ.3)DAY3=1

IOV=DAY1*ETA(5)+DAY2*ETA(6)+DAY3*ETA(7)

TVHILL=THETA(5)

HILL=TVHILL

TVTM50=THETA(6)

TM50=TVTM50

TVCL=THETA(1)

FSIZE=(WT/70)**0.75

FMAT=1/(1+(PMA/TM50)**(-HILL))

CL=TVCL*EXP(ETA(1))*EXP(IOV)*FSIZE*FMAT    ; clearance

TVV=THETA(2)

V=TVV*EXP(ETA(2))*(WT/70)          ; volume of distribution

Q=THETA(3)*EXP(ETA(4))*FSIZE*FMAT

V2=THETA(4)*EXP(ETA(3))*(WT/70)

;
```

K=CL/V

K12=Q/V

K21=Q/V2

;

S1=V

AUCCL=DOSE/CL

$DES

DADT(1) = -K*A(1)-K12*A(1)+K21*A(2)

DADT(2) = K12*A(1)-K21*A(2)

$ERROR

Y = F*(1+ERR(1))

IPRED=F

IRES=DV-IPRED

DEL=0

IF (IPRED.EQ.0) DEL=1

IWRES=(1-DEL)*IRES/(IPRED+DEL)

$THETA

(0, 18.8) ; TH_CL

(0, 20.2) ; TH_V

2

(0, 21.3) ; TH_Q

(0, 16.8) ; TH_V2

(0, 1.22) ; Hill

(0, 38) ; TM$_{50}$

$OMEGA BLOCK(4)

 0.101 ;   ET_CL

 0.131 0.211 ;   ET_Vc

 0.0349 0.026 0.0299 ;   ET_Vp

 -0.0307 -0.0354 -0.05 0.171 ;   ET_Q

$OMEGA BLOCK(1)

 0.0194

$OMEGA BLOCK(1) SAME

$OMEGA BLOCK(1) SAME

$SIGMA 0.0152 ; ER_Prop

$ESTIMATION METHOD=1 INTERACTION MAXEVAL=99999 PRINT=5 SIG=2 NOABORT POSTHOC MSFO=RFINAL8.nmv

$COVARIANCE unconditional matrix=s

$TABLE ID TIME DOSE IPRED IRES IWRES CL V ETA1 ETA2 IOV WT AGE CREAT

BSA ULD ULD2 COND TAD ISM CLCR AUCCL DAY ALB HB HT PH PMA EVID NOPRINT ONEHEADER FILE=RFINAL8.tab